Analysis of *P-P* and *P-SV* seismic data from Lousana, Alberta

Susan L.M. Miller, Mark P. Harrison*, Don C. Lawton, Robert R. Stewart, and Ken J. Szata**

ABSTRACT

Two orthogonal three-component seismic lines were shot by Unocal Canada Ltd. in January, 1987, over the Nisku Lousana Field in central Alberta. The purpose of the survey was to investigate a Nisku patch reef thought to be separated from the Nisku shelf to the east by an anhydrite basin. These data have been reprocessed and are currently being analyzed and used to develop methods for multicomponent seismic data analysis. The data are of overall good quality and major events were confidently correlated between the *P-P* and *P-SV* sections using offset synthetic seismograms. *P-SV* offset synthetic models were also used to extract interval *Vp/Vs* values from the *P-SV* data.

Forward log-based offset *P-P* and *P-SV* modelling shows character, isochron, and *Vp/Vs* variations associated with lithology and porosity changes between reservoir and non-reservoir rock in the Nisku. The modelling results indicate that multicomponent seismic analysis is applicable in carbonate settings, even when the reservoir intervals are relatively thin (23 m). To date, we have had difficulty applying the modelling results to this data set because of multiple contamination in the zone of interest and work is ongoing to resolve this issue. Full-waveform modelling is planned to better understand the multiple activity on both components. However, there are observable anomalies on the data which are currently under investigation.

Multicomponent recording provides additional seismic measurements of the subsurface to assist in developing an accurate geological model. Rock properties which can be extracted from elastic-wave data, such as *Vp/Vs*, reduce the uncertainty in predictions about mineralogy, porosity, and reservoir fluid type. Joint interpretation of *P-P* and *P-SV* data was helpful in horizon picking and in providing feedback on the validity of the interpretation. The interpretation techniques described in this paper can be usefully applied to other areas, including other carbonate plays.

INTRODUCTION

In 1987, Unocal acquired two three-component lines across the Lousana Field. Unocal donated these data to the CREWES Project, and in 1993 they were reprocessed using IT&A's software and converted-wave code developed in CREWES. More recently, the data were reprocessed again using the ProMAX processing package and the same converted-wave algorithms. The reprocessed sections exhibit significantly broader bandwidth on both the vertical and radial components. Modelling and interpretive studies are ongoing, with the following objectives:

* Sensor Geophysical Ltd., Calgary, Alberta
** Chevron Canada Resources, Calgary, Alberta

- identify character, amplitude, or time interval variations which may be associated with productive zones, and attempt to calibrate these variations to changes in geology through forward modeling,
- use full-waveform modelling to study the signal interference caused by interbed multi-converted multiples,
- develop and test techniques for analyzing multicomponent data,
- evaluate the benefit of multicomponent versus conventional recording.

Benefits of multicomponent recording

This discussion concentrates on the benefits of multicomponent recording as it applies to data interpretation. Recording multicomponent data provides complementary images of the subsurface for a relatively small additional cost, as conventional sources and receiver geometries are employed. Due to the difference in travel path, wavelength, and reflectivity, *P-SV* seismic sections may exhibit geologically significant changes in amplitude or character which are not apparent on conventional *P*-wave data. Horizons may be better imaged on one of the components because of different multiple paths and wavelet interference effects.

This additional seismic measurement of subsurface rock properties can reduce the uncertainty in predictions about mineralogy, porosity, and reservoir fluid type. The *P-SV* seismic data can be used in conjunction with the *P-P* data to determine other rock properties, such as *Vp/Vs* (or similarly, Poisson's ratio). *Vp/Vs* is sensitive to changes in a number of rock characteristics, including lithology, porosity, pore shape, and pore fluid (e.g. Pickett, 1963; Nations, 1974; Tatham, 1982; Eastwood and Castagna, 1983; Miller and Stewart, 1990). A number of studies, some of which are described below, have indicated that multicomponent seismic technology has practical applications in carbonate settings (Rafavich et al., 1984; Wilkens et al., 1984; Goldberg and Gant, 1988; Georgi et al., 1989; Wang et al., 1991).

Robertson (1987) interpreted porosity from seismic data by correlating an increase in porosity with an increase in *Vp/Vs*. He based his interpretation on the model of Kuster and Toksöz (1974), which incorporates pore aspect ratio as a factor in velocity response. According to this model, *Vp/Vs* will rise as porosity increases in a brine-saturated carbonate with flat pores, but will decrease slightly if the pores tend to have a higher aspect ratio (are rounder). If the carbonate is gas saturated, *Vp/Vs* will drop sharply as porosity increases if pores are flat, and drop slightly if pores are rounder.

Multicomponent data have been used successfully to differentiate tight limestone from reservoir dolomite in the Scipio Trend in Michigan. Pardus and others (1991) mapped the variation in the *Vp/Vs* ratio across the interval of interest on *P*- and *S*-wave seismic data and related it to the ratio of limestone to dolomite. Limestone tends to a *Vp/Vs* value of 1.9, dolomite of 1.8. Petrophysical studies suggest that anhydrite also has a higher *Vp/Vs* ratio than dolomite and thus might be used in a similar manner to track dolomite/anhydrite variations (Miller, 1992).

Finally, having two or more seismic measurements of the same geology gives the interpreter additional hard data to incorporate into the geological model. There is another data set to work with in areas where the data quality is poor or the interpretation is unclear. The *P-SV* section can be used to guide and constrain conventional data interpretation. Joint horizon interpretation offers the interpreter feedback in the form of the resultant interval *Vp/Vs* values. *Vp/Vs* values which lie outside the range expected

due to geological variations indicate mispicks, whereas reasonable values increase confidence in the interpretation.

Methods for multicomponent analysis

This paper discusses several techniques which are useful in the analysis of multicomponent seismic data. These can be summarized as:

- correlation of vertical and radial components through *P-P* and *P-SV* log-based offset synthetic modelling,
- matching *P-SV* offset synthetic seismograms to *P-SV* stacked seismic data and iteratively adjusting interval *Vp/Vs* values on the model to tie the data,
- workstation interpretation of horizons on *P-P* and *P-SV* components and calculation of interval *Vp/Vs* values using *P-P* and *P-SV* isochrons,
- log-based forward modelling to determine amplitude, character, and travel-time response of each component to a variety of geological settings,
- use of this model to determine the expected variation in *Vp/Vs* across different time intervals for a range of rock properties.

GEOLOGY

The Lousana field is located west of the Fenn-Big Valley and Stettler Oil Fields in Township 36, Range 21, West of the 4th Meridian, in central Alberta (Figure 1). The target is a Nisku dolomite buildup which is separated from the Nisku carbonate shelf to the east by an anhydrite basin, which forms the seal for the reef.

The Nisku is an Upper Devonian Formation in the Winterburn Group, which conformably overlies the shales and carbonates of the Woodbend Group (Figure 2). Immediately underlying the Nisku is the Ireton Formation, a calcareous shale. The initial deposition of the Nisku occurred during a relative rise in sea level. The antecedent topography of the Leduc reef complexes served as sites for deposition of the Nisku carbonates, which was concentrated in shallow waters. Deposition was restricted in deep-water areas to pinnacle reefs and small carbonate outliers (Stoakes, 1992).

During a later, regressive phase of deposition, sea water circulation was restricted by the growth of the shelf margin in the northwest, the current location of the West Pembina Field. Progressive evaporation resulted in the hypersaline deposits of an upper evaporitic unit in the Nisku. Brining upward cycles of dolomudstones and anhydrites infilled the lows between isolated reefs and platforms and capped the succession. Basin infilling was completed by the deposition of the silts and shales of the overlying Calmar Formation (Andrichuk and Wonfor, 1954).

The nearby Fenn West, Fenn-Big Valley, and Stettler Fields are structural traps formed by the porous dolomitized Nisku shelf carbonates draping over Leduc reefs (Rennie et al., 1989). There is no underlying Leduc at Lousana, which is west of the Leduc edge, and the stratigraphic trap is a biohermal buildup of dolomite, perhaps one of the carbonate outliers described by Stoakes (1992). The hypersaline deposits of the upper phase of the Nisku filled the basin between the shelf and the buildup at Lousana, and sealed the trap. The Nisku is 50 - 60 m thick in this area and the overlying Calmar Formation is generally only about 3 m thick.

The Nisku at Lousana is a dolomite oil reservoir with up to about 25 m of porosity in producing wells. The two oil wells in the field, 16-19-36-21W4 and 2-30-

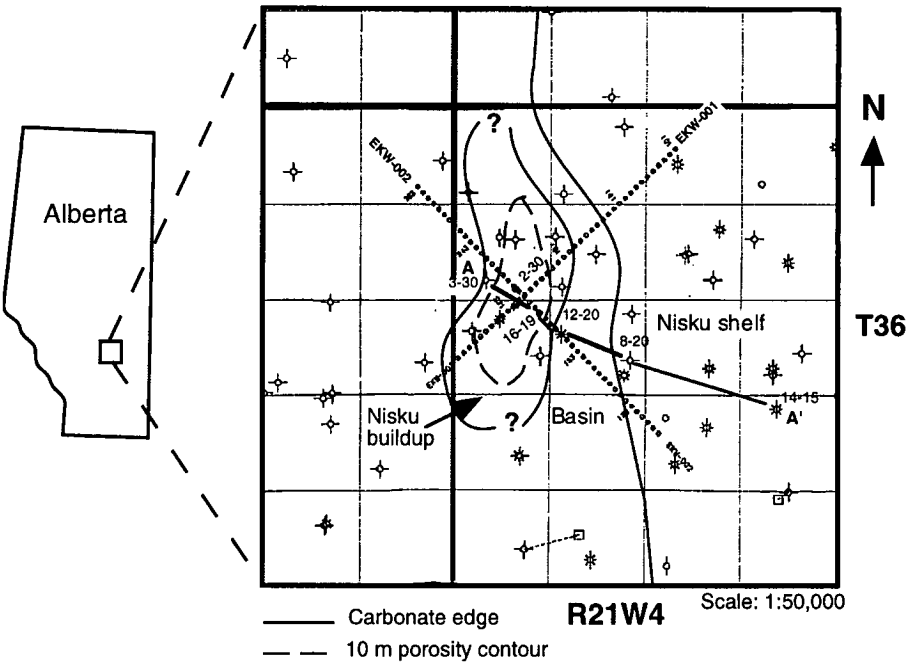

FIG. 1. Shotpoint map of the Lousana survey showing seismic lines EKW-001 and EKW-002, cross-section A-A', and well control. Carbonate edge and 10 m porosity contours are approximate only.

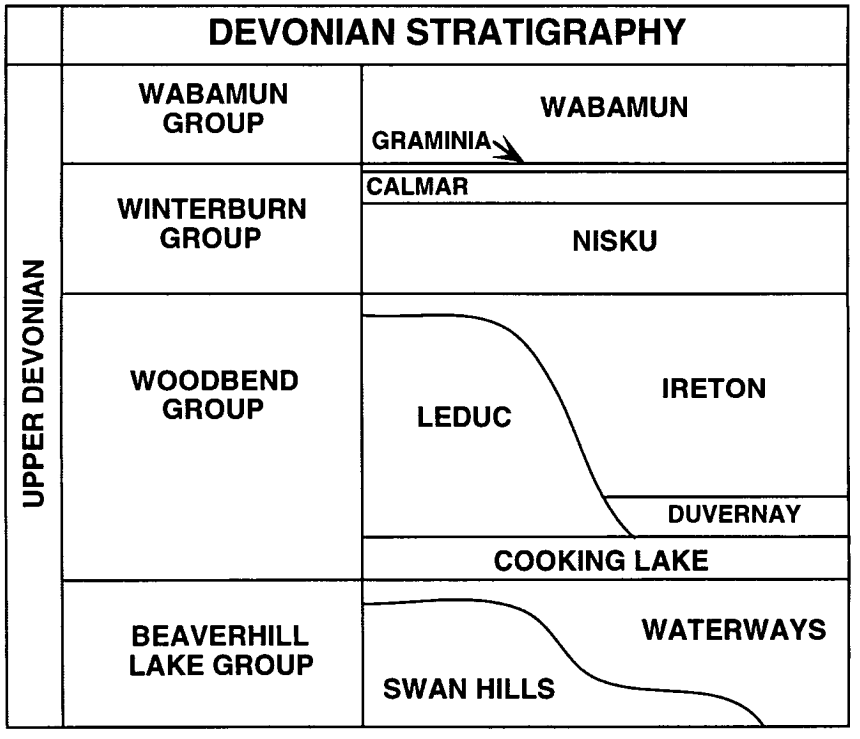

FIG.2. Stratigraphic chart of the Upper Devonian succession in central Alberta. (after Stoakes, 1979)

36-21W4, have about 25 m of porosity and 10 m of pay. The 16-19 well went on production in 1960 and has produced about 78,000 m^3 of oil. The 2-30 well has produced over 58,000 m^3 of oil since it went on production in 1962. The porosity is primarily vuggy, ranging to intergranular, and averages about 10% in the two producing wells. Dry holes in the field are either tight or wet carbonate, or massive anhydrite at the Nisku level. There is also gas production from the Viking and other Lower Cretaceous formations in this area.

Geological cross-section A-A', shown in Figure 3, roughly parallels line EKW-002, and is built from well logs from each of the shelf, basin, and reef environments.

DATA ACQUISITION AND PROCESSING

Data acquisition and processing are described in greater detail by Miller et al. (1993). The field acquisition parameters are summarized in Table 1. For both lines the geophones were oriented at 45 degrees to the line direction, giving comparable amounts of shear energy on H1 and H2. The H1 and H2 components were rotated into radial and transverse directions. Vertical-, radial-, and transverse-component gathers are shown in Figures 4, 5, and 6 respectively for one sourcepoint from each of the two lines. A time-variant gain function followed by individual trace-balance scaling has been applied to these field records. The radial-component records are seen to have good signal strength, with events that roughly correspond to those on the vertical component. There is little signal evident on the transverse component.

Table 1. Field acquisition and recording parameters for the Lousana survey.

Energy source	dynamite
Source pattern, EKW-001	single hole, 2 kg at 18 m
Source pattern, EKW-002	4 holes, 0.5 kg charges at 5 m
Amplifier type	2 - Sercel SN348
Number of channels	2 x 240
Sample rate	2 ms
Recording filter	Out-125 Hz
Notch filter	Out
Geophones per group	6 spread over 33 m
Type of geophones used	OYO 3-C, 10 Hz
Number of groups recorded	110
Group interval	33 m
Normal source interval	66 m
Nominal CMP fold	27
Spread	1799-16.5-SP-16.5-1799 m

The data were processed in 1993 on the IT&A system, as reported in Miller et al. (1993). Subsequent to that report, tests for the removal of multiples were performed using the parabolic radon transform method (Hampson, 1986) and predictive deconvolution. The results for both methods were inconsistent, with some portions of the data showing slight improvement while others were degraded.

The data have since been fully reprocessed on the ProMAX system using similar flows to the IT&A processing for both the vertical and radial components. Vertical and radial component flows are outlined in Figures 7 and 8 respectively. The final migrated stacked sections are shown in Figures 9-12.

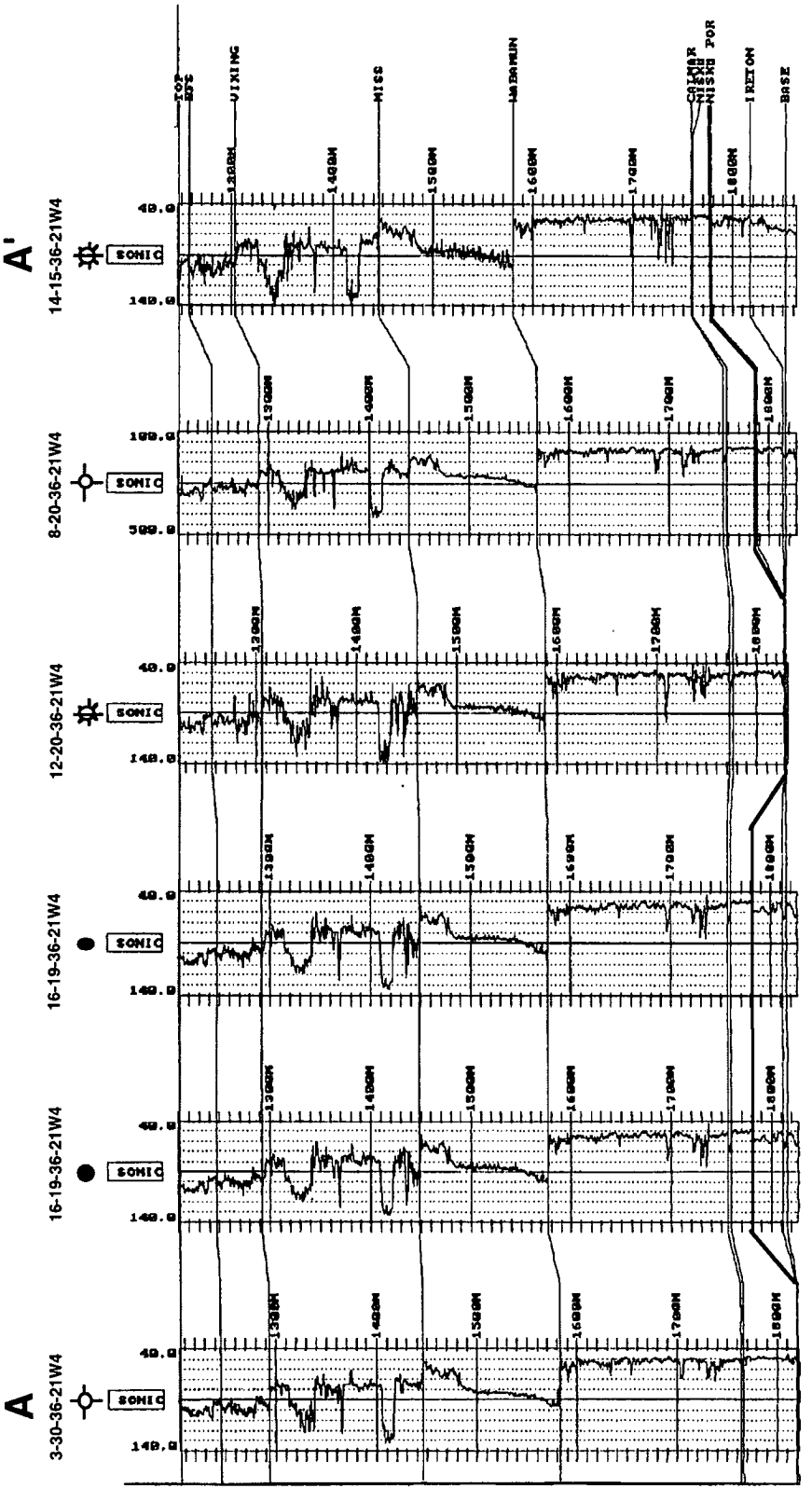

FIG. 3. Cross-section A-A', based on sonic logs from wells from the carbonate shelf (14-15, 8-20), anhydrite basin (12-20, 3-30), and porous reef (16-19) environments. 14-15 and 12-20 are suspended gas wells, with gas occuring in the Viking Formation. The 16-19 producing well is repeated as there is no sonic log for the nearby 2-30-36-21W4 oil well. The horizon named "NISKU POR" is the top of the porous dolomite in the Nisku Formation.

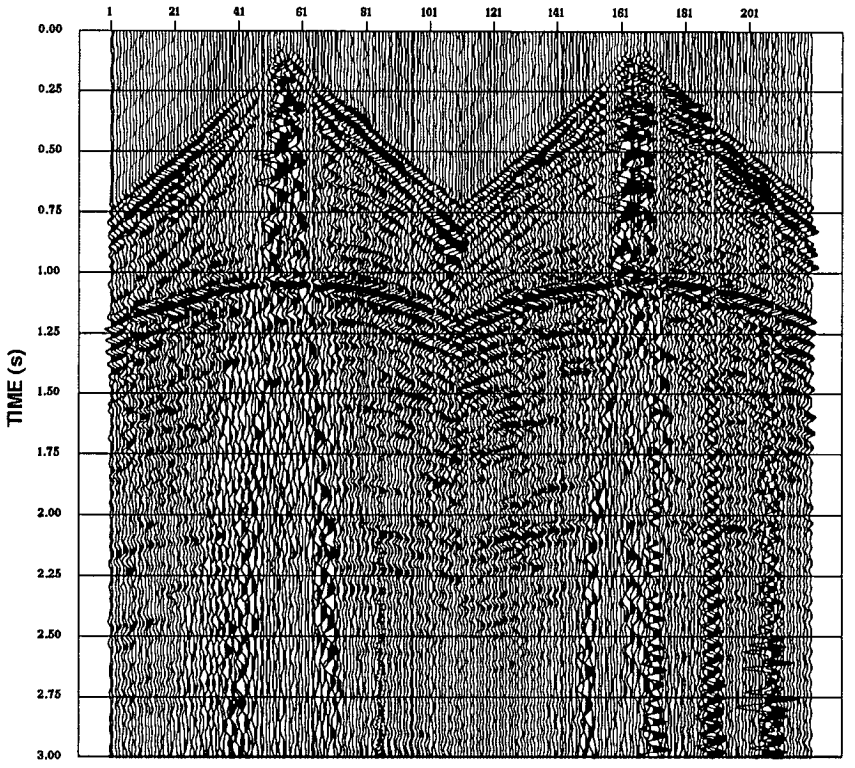

FIG. 4. Vertical-component records from line EKW-001, shotpoint 181.5 (left) and line EKW-002, shotpoint 185.5 (right).

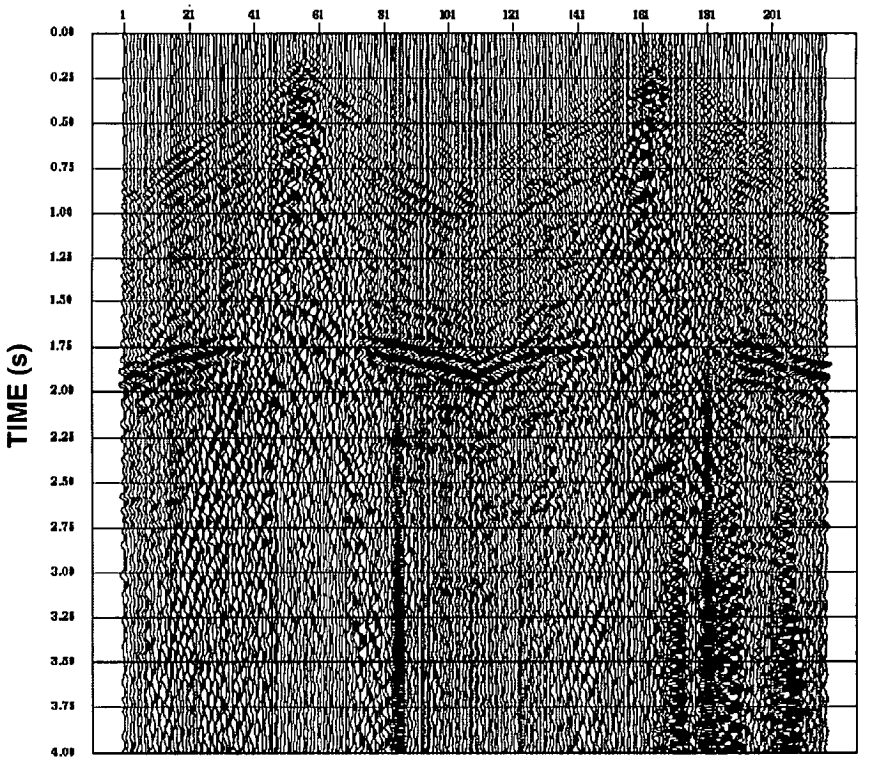

FIG. 5. Radial-component records from line EKW-001, shotpoint 181.5 (left) and line EKW-002, shotpoint 185.5 (right).

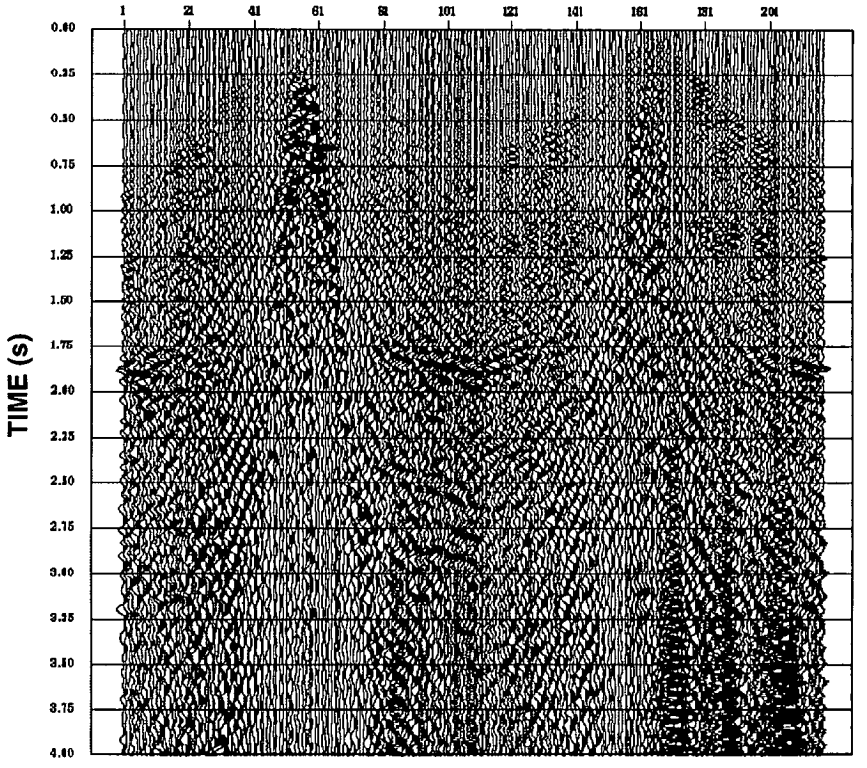

FIG. 6. Transverse-component records from line EKW-001, shotpoint 181.5 (left) and line EKW-002, shotpoint 185.5 (right).

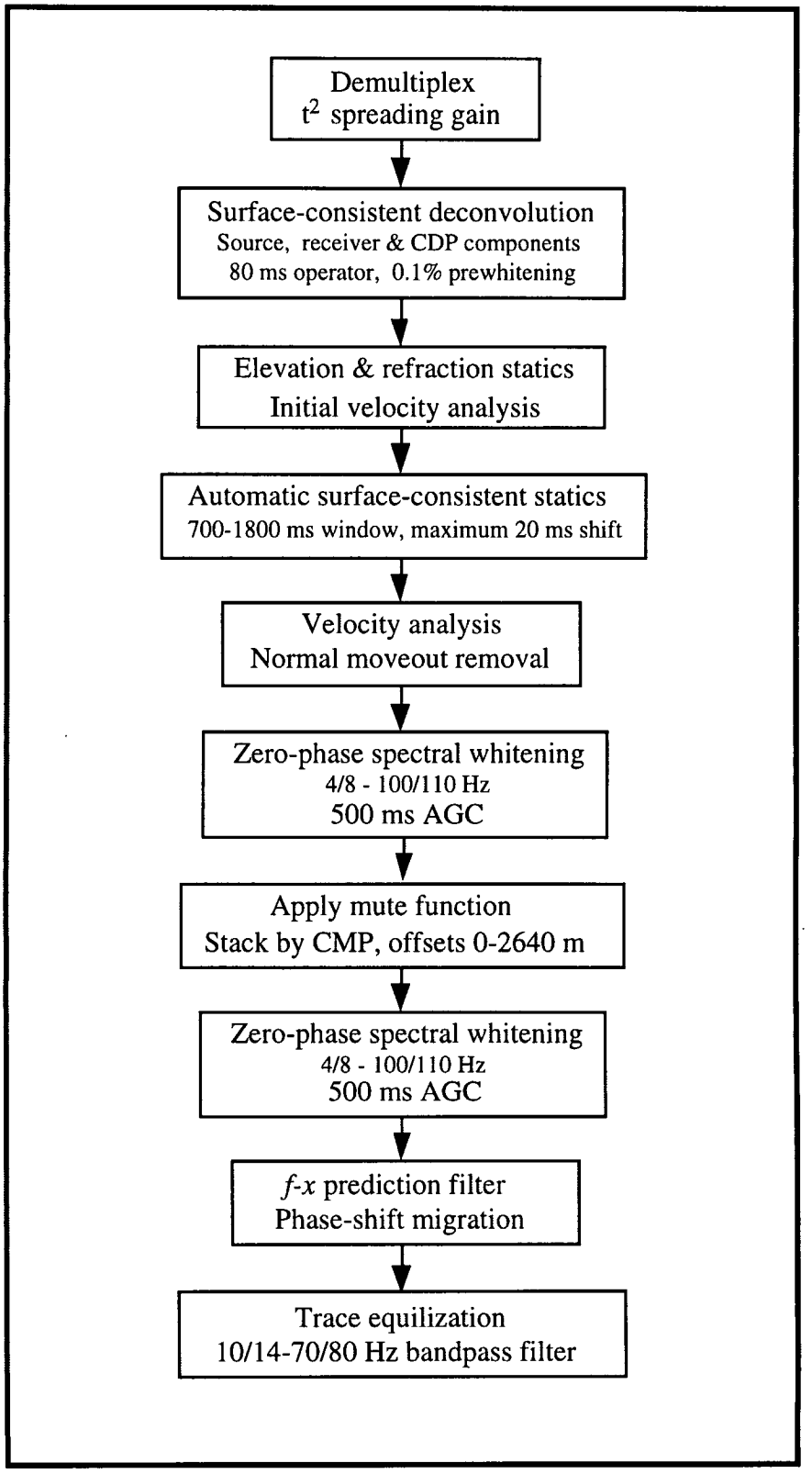

FIG. 7. Processing flow for vertical-component data.

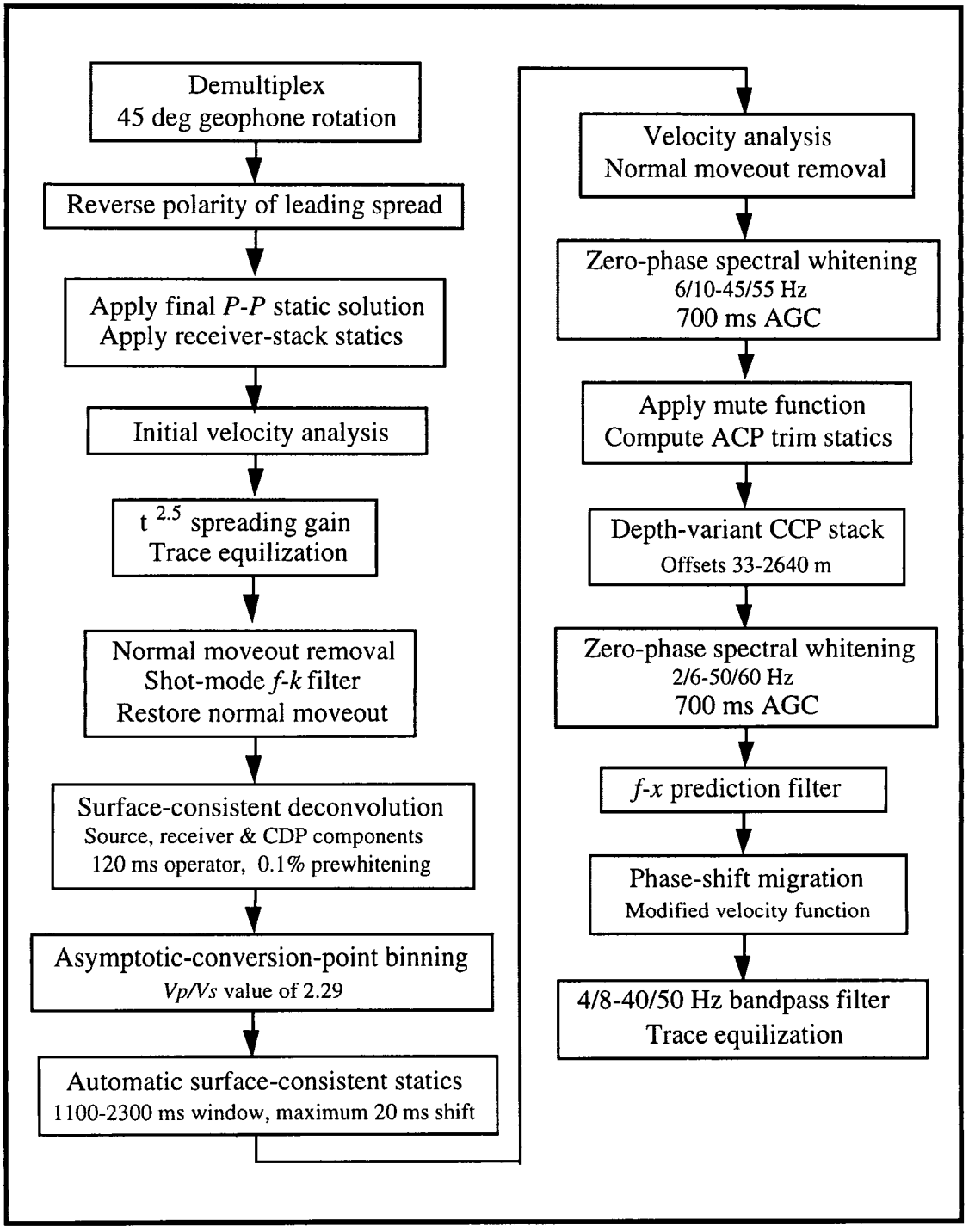

FIG. 8. Processing flow for radial-component data.

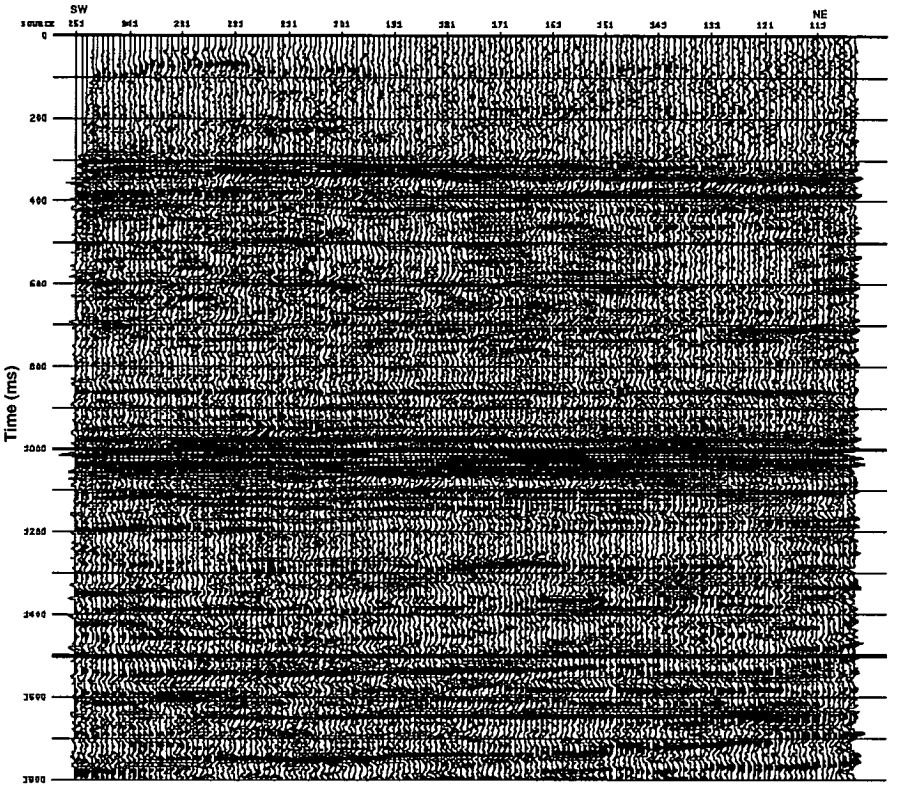

FIG. 9. Migrated *P-P* stacked section for line EKW-001 after reprocessing.

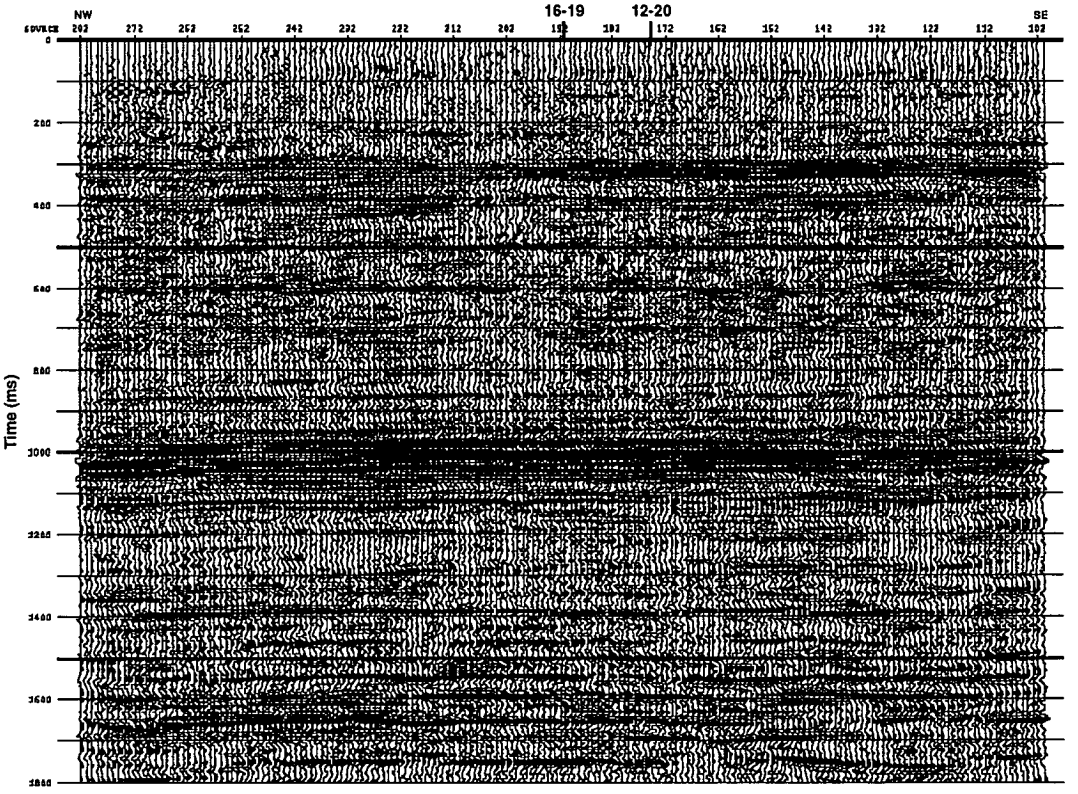

FIG. 10. Migrated *P-P* stacked section for line EKW-002 after reprocessing. The wells shown are used in correlation and modelling.

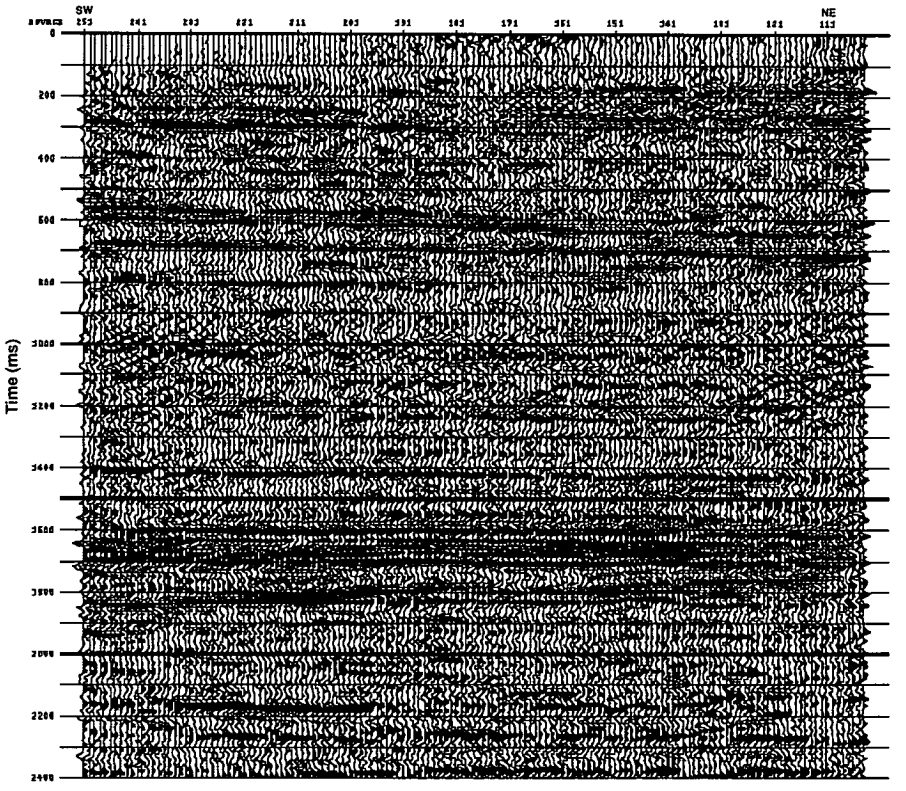

FIG. 11. Migrated *P-SV* stacked section for line EKW-001 after reprocessing.

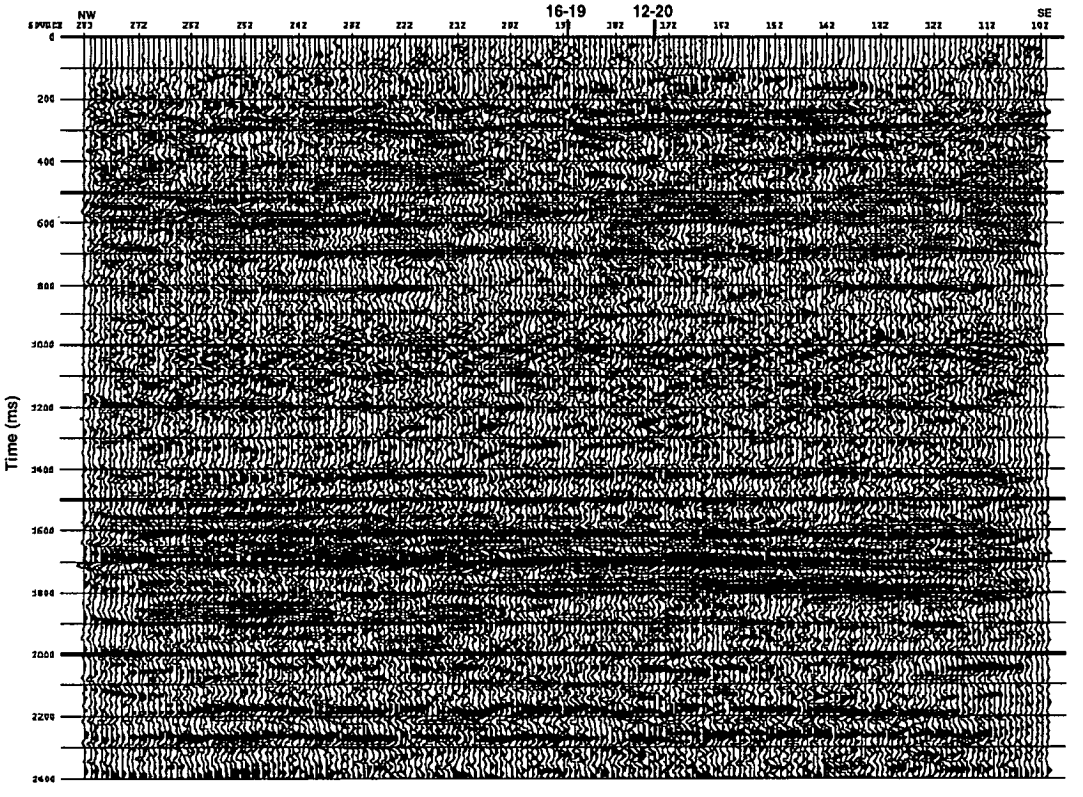

FIG. 12. Migrated *P-SV* stacked section for line EKW-002 after reprocessing. The wells shown are used in correlation and modelling.

For both components, the most recently processed data has significantly broader bandwidth. There is also improved imaging of some of the reflectors, most notably the Wabamun at about 1775 ms. Figure 13 shows a comparison of 1993 and 1994 processing on the radial component of line EKW-002.

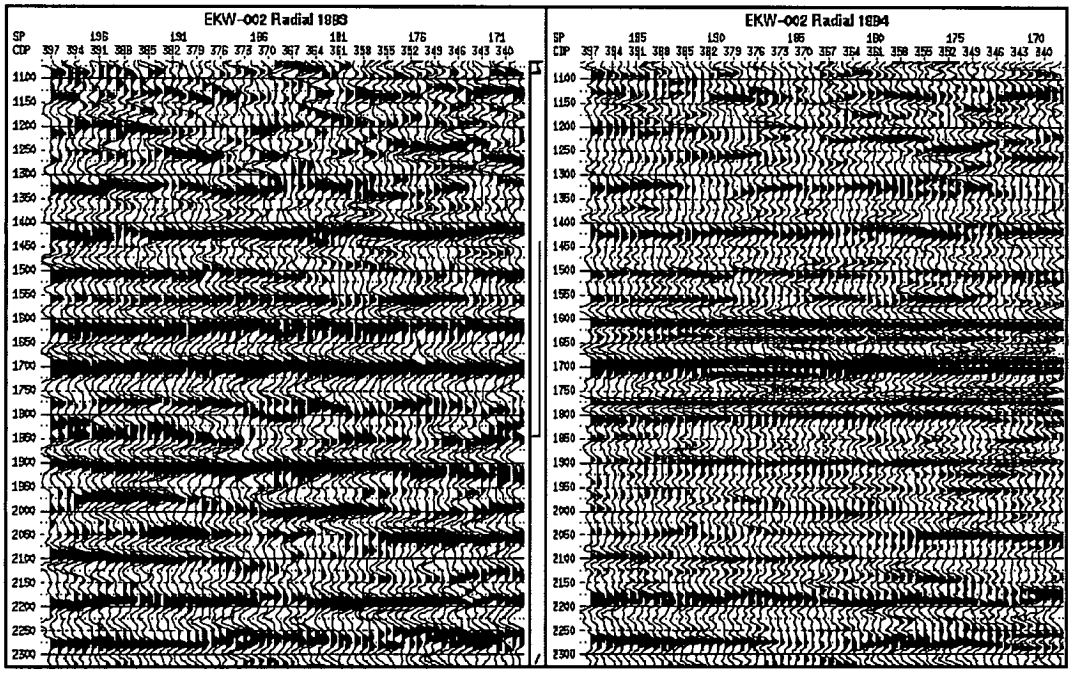

FIG. 13. Comparison of the radial component stacked section from line EKW-002 processed in 1993 (left) to the same data reprocessed in 1994 (right). In addition to the broader bandwidth, note the improved imaging of the Wabamun horizon, the peak at about 1775 ms. The peak at 1900 ms is the Nisku event.

MODELLING AND INTERPRETATION

Correlation of *P-P* and *P-SV* sections

Correlation between *P-P* and *P-SV* events was initially done on the IT&A-processed data, and did not need to be repeated for the data reprocessed on ProMAX. Thus, the figures in this section show data from the 1993 processing, but the technique applies to any data set.

Horizons were interpreted on the vertical (*P-P*) component in the conventional manner of matching a synthetic seismogram created from a sonic log to the seismic data. The data shown use the polarity convention that a peak represents a positive increase in acoustic impedance. The *P*-wave offset synthetic seismogram, from 16-19-36-21W4, matches the seismic very well through most of the section (Figure 14). However, the Wabamun, a high amplitude peak on the synthetic seismogram, is poorly imaged on the actual data. This is mostly likely due to interference from short path interbed multiples, probably originating in the coal beds of the Mannville Formation. This multiple energy also appears to interfere with the primary reflections from deeper in the section. A mistie occurs at the Nisku, causing uncertainty in the seismic pick for this horizon. Problems with the data quality below the Mississippian motivated the reprocessing of the data. The Wabamun event was improved on both components, particularly the *P-SV* data, but the Nisku mistie is still unresolved.

There are no full-waveform sonic logs or 3-C VSPs available from this area to serve as control for the *P-SV*, or radial component, interpretation. Therefore, offset *P-P* and *P-SV* synthetic seismograms were created from the 16-19 well, using the offset synthetic modelling program described by Lawton et al. (1992). Ricker wavelets were used, with a central frequency of 30 Hz for the *P-P* seismogram and 15 Hz for the *P-SV* seismogram. The offsets are from 0 to 1650 m, with a group interval of 66 m. Normal moveout corrections and mutes were applied prior to stacking the offset traces. For the initial correlation, the *P-SV* seismogram was calculated using the 16-19 sonic curve for the *P*-wave velocities and assuming a constant *Vp/Vs* of 2.00.

Our polarity convention is that a peak on the *P-SV* section represents an increase in acoustic impedance, as do peaks on the *P-P* data. Because both synthetic seismograms were created from the same depth model, the correlation between the offset synthetic stacks was straightforward. The *P-SV* synthetic seismogram was then used to identify the events on the *P-SV* seismic section (Figure 15).

Vp/Vs through offset synthetic modelling

Figure 15 indicates a time-variant shift between the events on the *P-SV* synthetic stack and the *P-SV* seismic data. This occurs because the synthetic model was created using a constant *Vp/Vs* value, whereas *Vp/Vs* varies with depth in the earth. The interval *Vp/Vs* can be adjusted to stretch or squeeze the synthetic stack in a time-variant manner such that the events line up with those on the data. To determine the correct interval *Vp/Vs*, a suite of *P-SV* offset synthetic stacks was generated using constant *Vp/Vs* values ranging from 1.60 to 2.20 in steps of 0.05 (Figure 16). *Vp/Vs* was taken from the synthetic stack which best fit the stacked section across a given interval. From this analysis, an *S*-wave transit time curve was generated from the *P*-wave sonic curve and the depth-variant *Vp/Vs* values. The final *P-SV* offset synthetic seismogram was generated using both *P*- and *S*-wave sonic curves and properly ties the *P-SV* data (Figure 17). The resultant interval *Vp/Vs* is interesting in that it is quite low in the Nisku to Cooking Lake interval, although the mistie at the Nisku horizon calls into question the validity of this result. Future plans include repeating this analysis on the newly reprocessed data.

Forward *P-P* and *P-SV* modelling

Well log curves were modified to simulate a variety of geologic conditions in the Nisku formation. The base *P*-wave sonic curve was from the 12-20-36-24W4 well which is on line EKW-002 (S.P. 175) and matched the *P*-wave seismic data reasonably well. The 12-20 well is in the basin with anhydrite at the Nisku level. This well only penetrated to the Ireton Fm, and so a composite curve was made using the 16-19-36-24W5 sonic log from the Ireton to the base at the Beaverhill Lake Fm. Since there was no density log available, the density log from 8-20-36-24W5 was modified to match the 12-20 depths. The values in Table 2 were used in the Nisku Formation to simulate anhydrite, tight limestone, tight dolomite, and dolomite with 10% porosity, both oil-filled and gas-filled. The values were obtained from well logs from the Lousana field, the Mobil Davey well at 3-13-34-29W4 (see Miller, 1992), Schlumberger (1989), and petrophysical relationships such as the time average equation (Wyllie et al., 1956). The Nisku porosity is primarily vuggy, so Roberston's Kuster-Toksöz models (1987) for rounded pores in dolomite were used to estimate the variation in *Vp/Vs* with porosity and pore fluid.

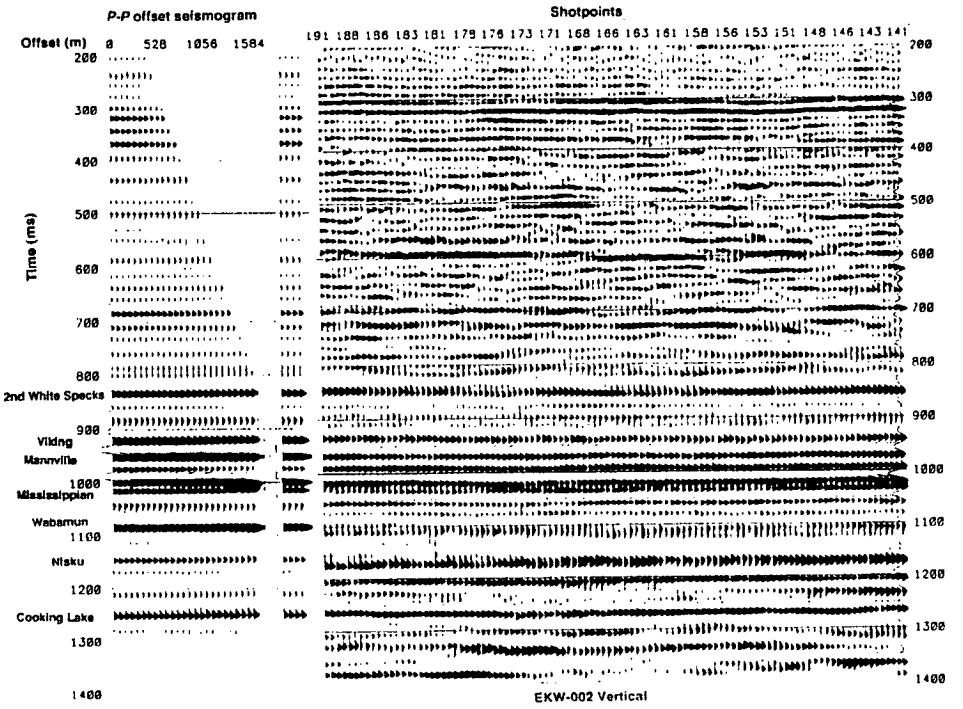

FIG. 14. Correlation of *P-P* offset synthetic seismogram and synthetic stack with *P-P* seismic data. The synthetic is generated from the 16-19 well, and spliced into line EKW-002 at S.P. 191. The tie is good except for the Wabamun and the mistie at the Nisku. The seismic data were processed using IT&A software.

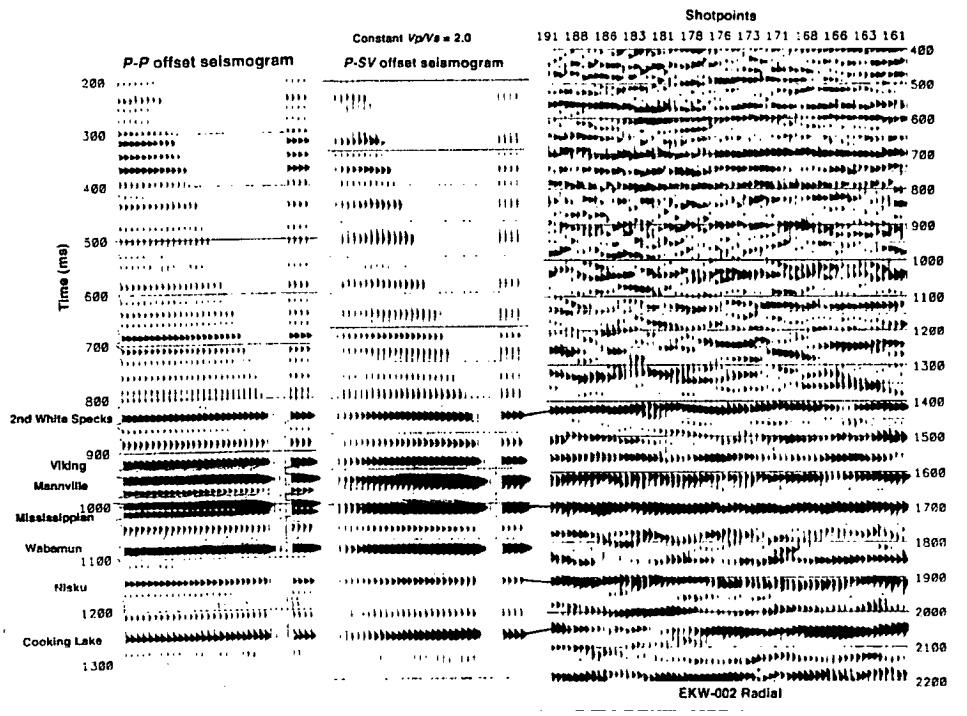

FIG. 15. The *P-P* seismogram is first tied to the *P-SV* seismogram, which was generated using the *P*-wave sonic log from 16-19 and a constant *Vp/Vs* of 2.0. It is plotted at 2/3 the scale of the *P-P* seismogram. The *P-SV* seismogram is then tied to the *P-SV* data at shotpoint 191. The correlation is straight forward, but there are time misties due to the assumption of constant *Vp/Vs*. Processing was on IT&A's software.

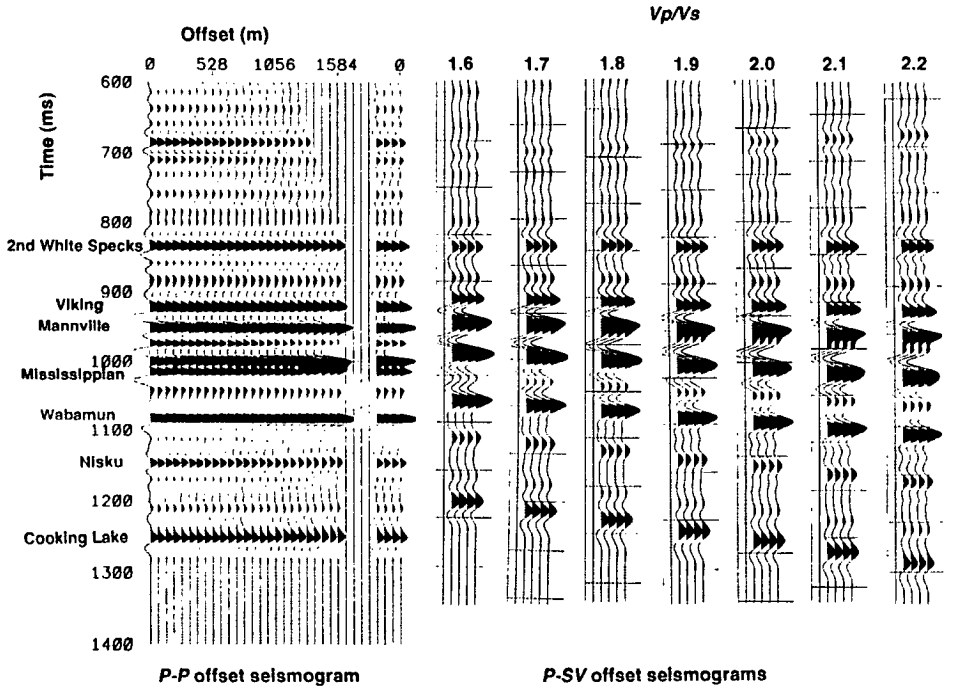

FIG. 16. The *P-P* offset synthetic seismogram and stack is compared to a series of *P-SV* offset synthetic stacks. *P-SV* stacks were generated using the *P*-wave sonic log from 16-19 and constant *Vp/Vs* values ranging from 1.60 to 2.20 in steps of 0.05; every other one is shown here. The seismogram stretches in time as *Vp/Vs* is increased.

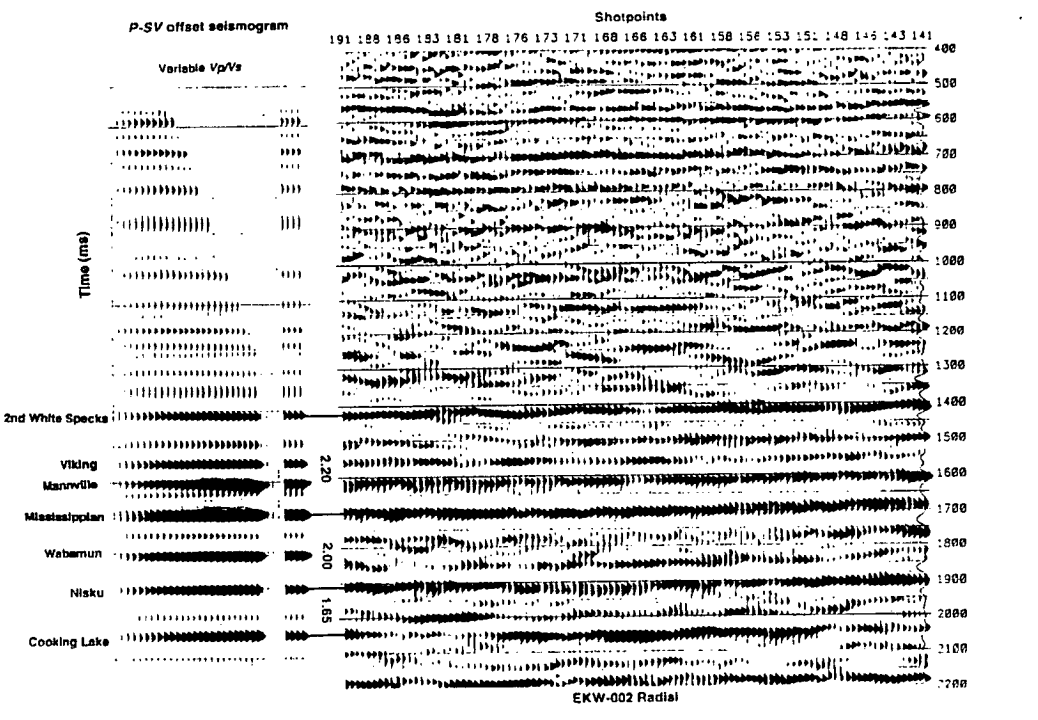

FIG. 17. *P-SV* synthetic stacks from Figure 16 were compared to the *P-SV* data to determine optimum interval*Vp/Vs* values. The interval *Vp/Vs* values were used to generate a new *S*-wave sonic curve for input to the *P-SV* synthetic seismogram. The resultant *P-SV* seismogram shown here ties the data correctly. In this case, the mistie at the Nisku (Figure 14) still causes some uncertainty in the results.

Table 2. Rock property values used in *P-P* and *P-SV* offset synthetic models.

	Δt_p (μs/ft) [μs/m]	Δt_s (μs/ft) [μs/m]	*Vp/Vs*	density (g/cm^3) [kg/m^3]
Anhydrite	50 [164]	100[328]	2.00	2.96 [2960]
Tight limestone	47 [154]	90 [295]	1.90	2.70 [2700]
Tight dolomite	43 [141]	77 [253]	1.80	2.85 [2850]
Dolomite: 10% porosity - oil filled	57 [187]	100[328]	1.75	2.65 [2650]
Dolomite: 10% porosity - gas filled	65 [213]	100 [328]	1.55	2.56 [2560]

The Nisku interval is 162 ft (50 m) thick, from 5828 to 5990 ft (1776-1826 m). Two porosity thicknesses were simulated: 75 ft (23 m) from 5900 to 5975 ft (1798-1821 m) as is found in the 16-19 well, and 125 ft (38 m) from 5850-5975 ft (1783-1821 m) where depths are relative to kelly bushing. The porosity was overlain by anhydrite and underlain by tight dolomite within the Nisku. All the logs are identical outside of the Nisku formation.

The *P-P* model consisted of 25 receivers with 66 m spacing, with a far offset of 1650 m. Because of phase changes at far offsets, the spread was reduced for the *P-SV* model to 22 receivers at 66 m spacing for a far offset of 1452 m. A 40 Hz zero-phase Ricker wavelet was used for the *P-P* model and a 25 Hz zero-phase Ricker for the *P-SV* model to best match the reprocessed data.

The offset synthetic stacks are shown for the *P-P* case in Figure 18 and the *P-SV* case in Figure 19. Both components exhibit changes at the Nisku level with changes in lithology, porosity, and pore fluid. When porosity is introduced, a trough followed by a peak develops below the peak at the top of the Nisku, indicating porosity and the base of porosity respectively. The amplitude of this lower peak brightens either by thickening the porosity from 23 m to 38 m or by the replacement of oil with gas. The modelled *P-P* response is similar for anhydrite and tight limestone: a tight doublet. A slight difference in the character of the doublet is evident on the *P-SV* model. In tight dolomite a single broad peak/trough pair is evident on both models.

Horizons were picked on both models and *P-P* and *P-SV* isochrons used to calculate *Vp/Vs* values across several time intervals for each stack. For converted-wave data, *Vp/Vs* is equivalent to (2Is/Ip) -1, where Is and Ip are the *P-SV* and *P-P* interval transit times respectively (Garotta, 1987). Horizons were chosen which bracketed the Nisku and can be readily identified on the real data. Figures 20 and 21 show *Vp/Vs* variations across six intervals with the following thicknesses:

Mississippian - Cooking Lake:	1906 ft	581 m
Wabamun - Cooking Lake:	1484 ft	452 m
Wabamun salt marker - Cooking Lake:	1076 ft	328 m
Mississippian - Ireton trough:	1200 ft	366 m
Wabamun - Ireton trough:	778 ft	237 m
Wabamun salt marker - Ireton trough:	370 ft	113 m

There are several observations to note from these plots. *Vp/Vs* varies with lithology, porosity, and pore fluid, with the degree of variation diminishing as the thickness of the interval increases. The general trend is for *Vp/Vs* to decrease to the right as the model changes from nonreservoir rocks to reservoir rocks. Thickening the porous zone from 23 m to 38 m decreases *Vp/Vs* more than replacing the oil with gas.

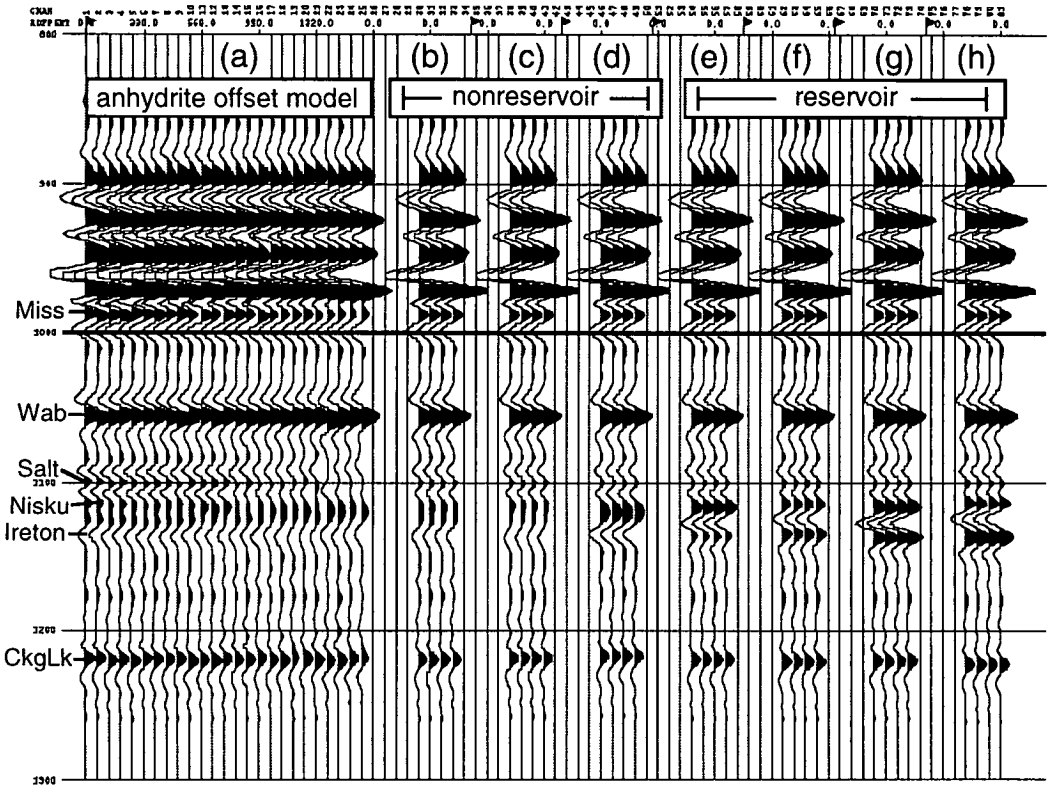

FIG. 18. *P-P* model results showing (a) offset synthetic seismogram for anhydrite, and offset synthetic stacks for (b) anhydrite; (c) tight limestone; (d) tight dolomite; (e) 23 m oil-filled porous dolomite; (f) 38 m oil-filled porous dolomite; (g) 23 m gas-filled porous dolomite; (h) 38 m gas-filled porous dolomite.

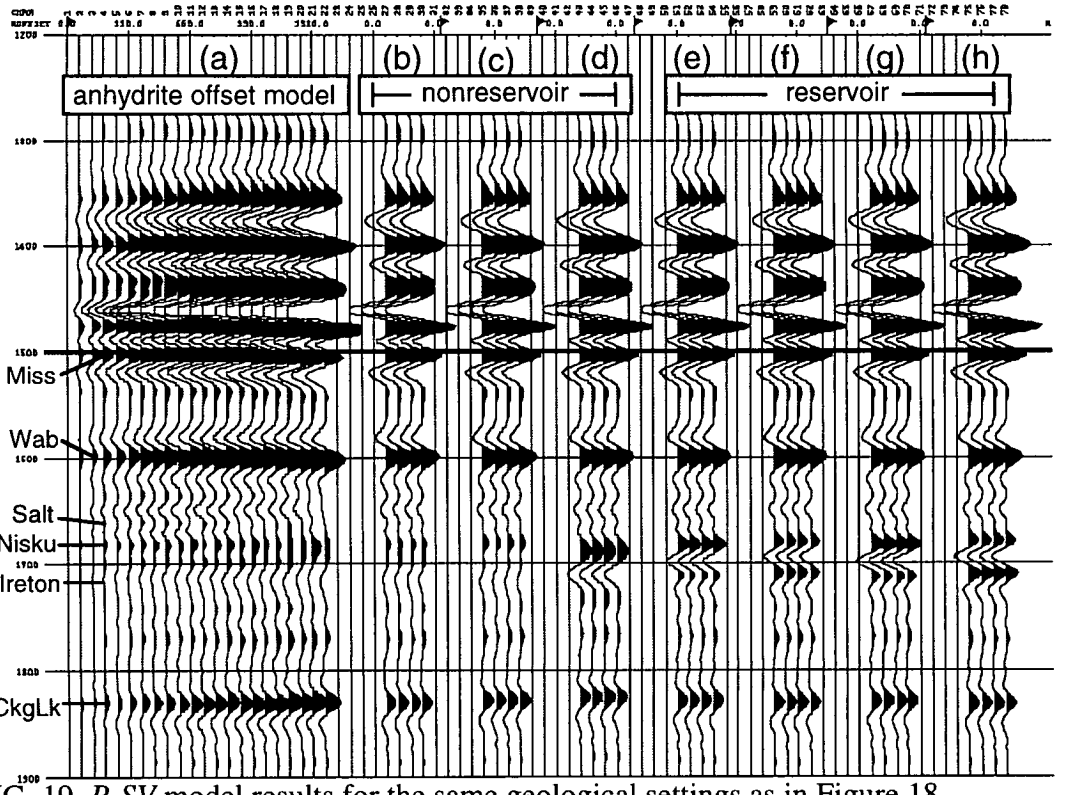

FIG. 19. *P-SV* model results for the same geological settings as in Figure 18.

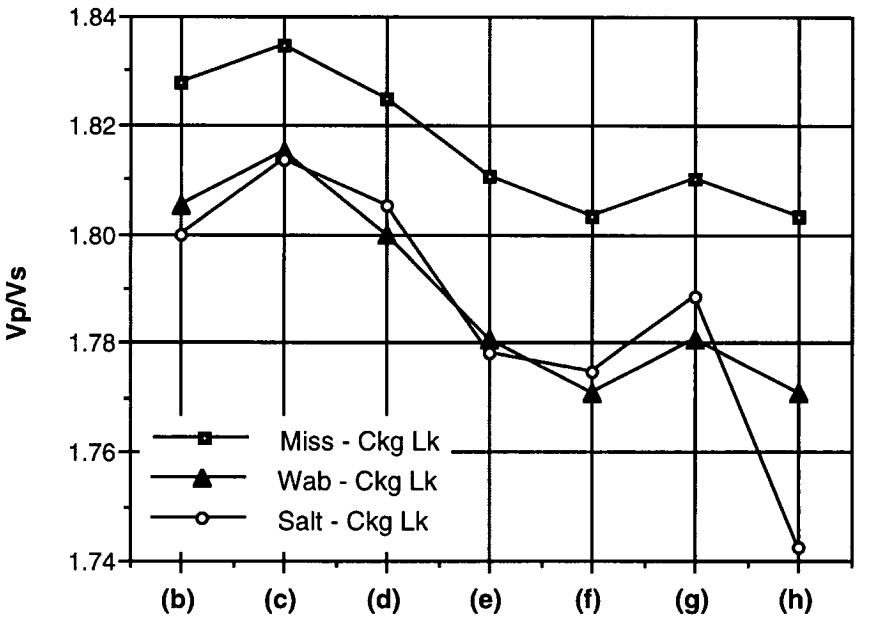

FIG. 20. Plot of Vp/Vs measured across intervals on the model data in Figures 18 & 19. The lower horizon is the Cooking Lake (Ckg Lk) and the upper horizons are the Mississippian (Miss), Wabamun (Wab), and Wabamun salt marker (Salt). The Nisku simulates (b) anhydrite; (c) tight limestone; (d) tight dolomite; (e) 23 m oil-filled porous dolomite; (f) 38 m oil-filled porous dolomite; (g) 23 m gas-filled porous dolomite; (h) 38 m gas-filled porous dolomite.

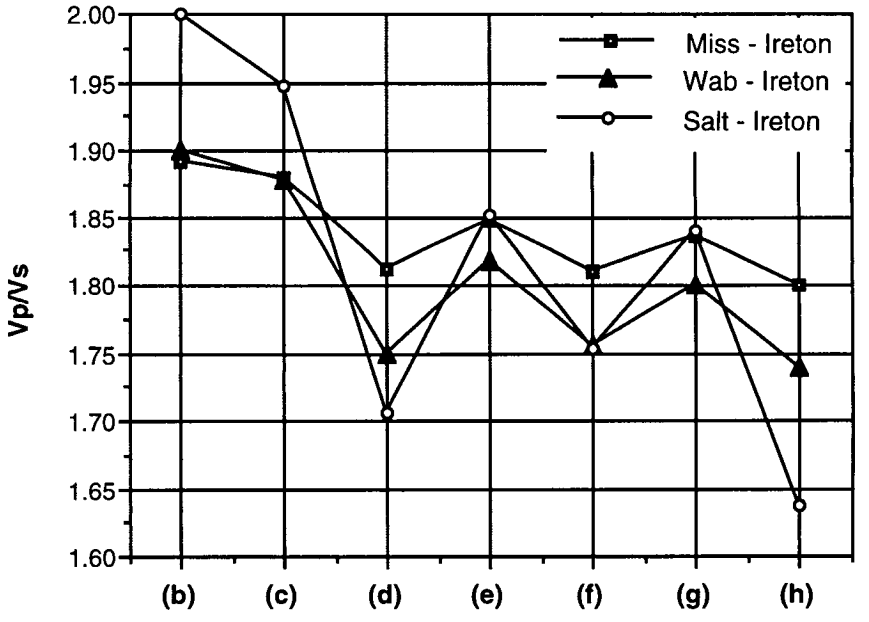

FIG. 21. Plot of Vp/Vs measured across three more intervals on the model data with the Ireton as the lower horizon. The upper horizons and the geological settings are the same as in Figure 20.

If one of the bounding horizons is too close to the zone of interest, wavelet interference from that zone may affect the picks and cause unexpected results. This is probably the case for the sharp decrease in *Vp/Vs* which occurs for tight dolomite when the bottom horizon is the Ireton, which underlies the Nisku. This may also be the cause of the increase in *Vp/Vs* across the Wabamun salt to Cooking Lake interval when gas replaces oil with 23 m of porosity. Using this salt as the top marker and the Ireton as the base marker produces the thinnest interval and thus the largest variations in *Vp/Vs*, however the values may be in error due to wavelet interference.

Our experience is that changes of 0.05 in *Vp/Vs* are observable on seismic sections. The intervals which use the Ireton as the lower bounding horizon show at least this much change between the anhydrite and 23 m of porous dolomite (as occurs in the oil wells). This suggests that the difference may be detectable on seismic data, although possible wavelet interference from the Nisku should be considered. The greatest contrast for all intervals occurs between tight anhydrite or limestone and the 38 m thick gas-filled porous dolomite. This effect might be observable even in oil plays if the gas to oil ratio is high enough. Gas saturation as low as 5-10% will result in a sharp decrease in *Vp/Vs* (Gregory, 1977). The modelling results indicate that *Vp/Vs* analysis is applicable in carbonate settings, even when the reservoir intervals are relatively thin (23 m) and comprise only 15-20% of the total measured interval.

Workstation interpretation

The reprocessed migrated sections of both components were loaded onto the Landmark workstation and the correlated events interpreted on both lines. Interpretation of the new data is in progress, but *P-P* and *P-SV* interpretations to date for line EKW-002 are shown in Figure 22. The *P-SV* data are plotted at 2/3 the scale of the *P-P* data, and the excellent tie between the two components is evident.

Isochrons and *Vp/Vs* ratios were calculated for several intervals between the interpreted horizons. If the event correlations between the components are accurate, the dimensionless ratio will be free of effects due to depth or thickness variations, as these will affect both components equally. Variations may be caused by factors such as changes in lithology, porosity, pore fluid, and other formation characteristics (Tatham and McCormack, 1991).

Figure 23 shows *Vp/Vs* along line EKW-002 for two intervals. The top curve is the interval *Vp/Vs* for the portion of the Cretaceous section from the Second White Specks to the Mannville. The high *Vp/Vs* values from about 2.2 to 2.4 are consistent with a shaley section. By contrast, the *Vp/Vs* values from an interval within the Paleozoic, the Mississippian to the Nisku, average about 1.8, a reasonable value for carbonate rocks. In the Paleozoic interval, *Vp/Vs* decreases to about 1.6 between shotpoints 182 and 202. Examination of the isochrons shows a thickening of the isochron on the *P-P* data and a thinning on the *P-SV* data, both contributing to the overall drop in *Vp/Vs*. The 16-19 well at shotpoint 191 is located on a structural high, suggesting that the *P-SV* time structure is consistent with the geological structure. Pushdown of the Nisku horizon on the *P-P* section may be a velocity effect caused by features in the shallower part of the section. This *Vp/Vs* anomaly occurs in the section immediately above, but not including, the Nisku reservoir. With further analysis we hope to determine if it is related to the dolomitic buildup in the underlying section.

To date, we have been unable to measure *Vp/Vs* across an interval which includes the Nisku reservoir. Several of the horizons which bound the Nisku have been damaged by multiple interference and cannot be picked with the level of certainty required for meaningful results. We are still working with the data

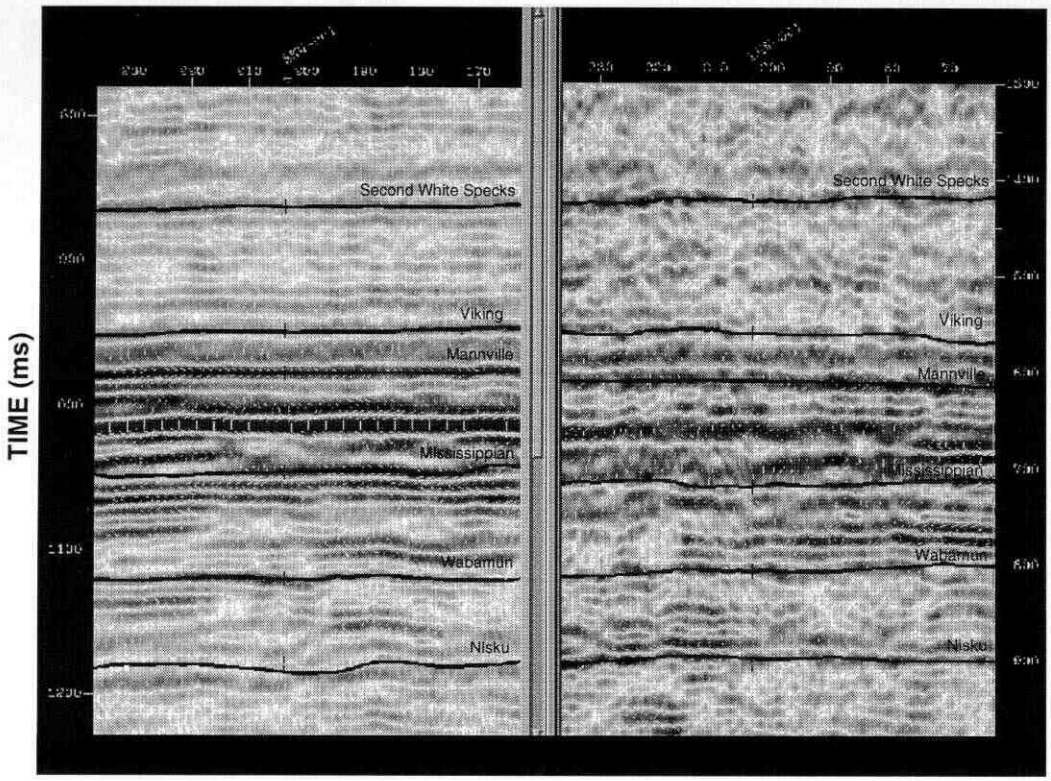

FIG. 22. Interpretation of the *P-P* data (left) and *P-SV* data (right) is shown for part of line EKW-002. To facilitate interpretation, the sections are displayed on the workstation simultaneously and the *P-SV* data plotted at 2/3 the scale of the *P-P* data.

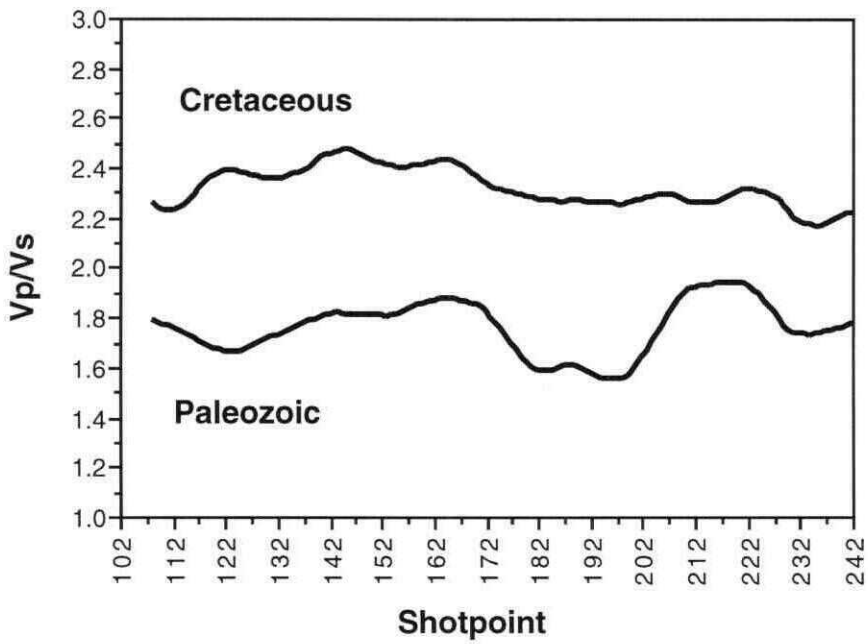

FIG. 23. *Vp/Vs* values on line EKW-002 for two intervals: Second White Specks to Mannville in the Cretaceous section and Mississippian to Nisku in the Paleozoic. This Cretaceous interval is primarily shales, whereas the Paleozoic consists mainly of carbonate rocks. The difference in lithology is reflected in *Vp/Vs*.

in an attempt to use horizons which bound the Nisku and can be picked with a reasonable level of confidence.

The advantages of having two seismic data sets to work with became evident during the course of this study. It was useful to display both components on the screen simultaneously while picking horizons, especially in zones where the horizons were difficult to track. In the case of the Wabamun and Nisku horizons, the pick was clearer on the *P-SV* data than on the *P-P* data. Also, the calculated *Vp/Vs* values were used as a quality control check on the horizon interpretations. *Vp/Vs* values which were outside the range expected due to geological variations indicated mispicks and the need to revisit the data. For example, on both components there were two possible picks for the Wabamun event. Choosing the wrong cycle on either section resulted in unreasonable *Vp/Vs* values for the intervals above and below the pick. *Vp/Vs* provided a useful constraint on the interpretation of this and other horizons. By providing the interpreter with feedback on the validity of horizon picks, *Vp/Vs* can increase confidence in the final interpretation.

SUMMARY

Two orthogonal three-component seismic lines were shot by Unocal in January, 1987, over the Nisku Lousana Field in central Alberta. The purpose of the survey was to investigate a Nisku patch reef thought to be separated from the Nisku shelf to the east by an anhydrite basin. These data have been reprocessed and are currently being analyzed and used to develop methods of multicomponent seismic data analysis. Several techniques which are useful in the analysis of multicomponent data are described and applied in this study. The data are of overall good quality and major events were confidently correlated between the *P-P* and *P-SV* sections using offset synthetic seismograms. *P-SV* offset synthetic modelling was also used to extract interval *Vp/Vs* values from the *P-SV* data.

Forward offset synthetic modelling showed character, isochron, and *Vp/Vs* variations associated with changes in lithology, porosity, porosity thickness, and pore fluid. The modelling results indicate that multicomponent seismic analysis is applicable in carbonate settings, even when the reservoir intervals are relatively thin (23 m) and comprise only 15-20% of the total measured interval. To date, we have had difficulty applying these results to this data set because of multiple contamination in the zone of interest, however work is ongoing to resolve this issue.

Multicomponent recording provides additional seismic measurements of the subsurface to assist in developing an accurate geological model. Rock properties which can be extracted from elastic-wave data, such as *Vp/Vs*, reduce the uncertainty in predictions about mineralogy, porosity, and reservoir fluid type. Joint interpretation of *P-P* and *P-SV* data was helpful in horizon picking and in providing feedback on the validity of the interpretation. The interpretation techniques described in this paper can be usefully applied to other areas, including other carbonate plays.

FUTURE WORK

The results of forward modelling encourage us to continue working with this data set. We hope to obtain further results from interpretation methods described in this paper, such as interval *Vp/Vs* analysis. Multiple contamination has complicated the application of these methods, so we plan to pursue full-waveform modelling to try to

understand the effects of interbed multiple energy on both components. Continued AVO modelling and AVO inversion may help us further understand the effects of mineralogy, porosity, and pore fluid in carbonate settings. In keeping with our objective to develop multicomponent interpretation techniques, we plan to enhance the offset synthetic modelling program as a tool for extracting interval *Vp/Vs* values.

ACKNOWLEDGMENTS

We would like to acknowledge Unocal Canada Ltd. for donating the seismic data to the CREWES Project. We are grateful to Chevron Canada Resources and Sensor Geophysical Ltd. for participating in this study, particularly for the time and effort spent by Mark Harrison on reprocessing the data at the University of Calgary. Our thanks to the companies which donated software used in this work: Landmark, GMA, and Hampson-Russell. Thank you to Andrea Bell of Norcen Energy Resources Ltd. for useful discussions on the geology of the Lousana Field. We thank the CREWES Sponsors for their financial support.

REFERENCES

Andrichuk, J.M. and Wonfor, J.S., 1954, Late Devonian geologic history in Stettler area, Alberta, Canada: AAPG Bull., 38, 2500-2536.

Domenico, S.N., 1984, Rock lithology and porosity determination from shear and compressional wave velocity: Geophysics, 49, 1188-1195.

Eastwood, R.L. and Castagna, J.P., 1983, Basis for interpretation of *Vp/Vs* ratios in complex lithologies: Soc. Prof. Well Log Analysts 24th Annual Logging Symp.

Garotta, R., 1987, Two-component acquisition as a routine procedure, *in* Danbom, S.H., and Domenico, S.N., Eds., Shear-wave exploration: Soc. Expl. Geophys., Geophysical development series 1, 122-136.

Georgi, D.T., Heavysege, R.G., Chen, S.T., and Eriksen, E.A., 1989, Application of shear and compressional transit-time data to cased hole carbonate reservoir evaluation: Can. Well Logging Soc. 12th Formation Evaluation Symp.

Goldberg, D. and Gant, W.T., 1988, Shear-wave processing of sonic log waveforms in a limestone reservoir: Geophysics, 53, 668-676.

Gregory, A.R., 1977, Aspects of rock physics from laboratory and log data that are important to seismic interpretation, *in* Seismic Stratigraphy - Applications to Hydrocarbon Exploration: AAPG Memoir 26, 15-45.

Hampson, D., 1986, Inverse velocity stacking for multiple elimination: Can. J. Expl. Geophys., 22, 44-45.

Kuster, G.T. and Toksöz, M.N., 1974, Velocity and attenuation of seismic waves in two-phase media: Part 1. Theoretical formulations: Geophysics, 39, 587-606.

Lawton, D.C. and Howell, C.E., 1992, *P-SV* and *P-P* synthetic stacks: Presented at the 62th Annual SEG Meeting.

Miller, S.L.M. and Stewart, R.R., 1990, Effects of lithology, porosity and shaliness on *P*- and *S*-wave velocities from sonic logs: Can. J. Expl. Geophys., 26, 94-103.

Miller, S.L.M., 1992, Well log analysis of *Vp* and *Vs* in carbonates: CREWES Research Report 4.

Miller, S.L.M., Harrison, M.P., Szata, K.J., and Stewart, R.R., 1993, Processing and preliminary interpretation of multicomponent seismic data from Lousana, Alberta: CREWES Research Report 5.

Nations, J.F., 1974, Lithology and porosity from acoustic shear and compressional wave transit time relationships: Soc. Prof. Well Log Analysts 15th Annual Symp.

Pardus, Y.C., Conner, J., Schuler, N.R., and Tatham, R.H., 1990, *Vp/Vs* and lithology in carbonate rocks: A case study in the Scipio trend in southern Michigan: Presented at the 60th Annual SEG Meeting.

Pickett, G.R., 1963, Acoustic character logs and their applications in formation evaluation: J. Petr.Tech., June, 659-667.

Rafavich, F., Kendall, C.H.St.C., and Todd, T.P., 1984, The relationship between acoustic properties and the petrographic character of carbonate rocks: Geophysics, 49, 1622-1636.

Rennie, W., Leyland, W., and Skuce, A., 1989, Winterburn (Nisku) Reservoirs *in* Anderson, N.L., Hills, L.V., and Cederwall, D.A., Eds. The CSEG/CSPG Geophysical Atlas of Western Canadian Hydrocarbon Pools, 133-154.

Robertson, J.D., 1987, Carbonate porosity from S/P traveltime ratios: Geophysics, 52, 1346-1354.

Schlumberger, 1989, Log Interpretation Principles/Applications: Schlumberger Educational Services.

Stoakes, F.A., 1979, Sea level control of carbonate-shale deposition during progradational basin-filling: the Upper Devonian Duvernay and Ireton Formations of Alberta, Canada: Ph.D. dissertation, Univ. of Calgary.

Stoakes, F.A., 1992, Winterburn megasequence *in* Wendte, J., Stoakes, F.A., Campbell, C.V., Devonian-Early Mississippian carbonates of the Western Canada sedimentary basin; a sequence stratigraphic framework: SEPM short course No. 28, 207-224.

Tatham, R.H., 1982, *Vp/Vs* and lithology: Geophysics, 47, 336-344.

Tatham,R.H. and McCormack, M.D., 1991, Multicomponent Seismology in Petroleum Exploration: Soc. Expl. Geophys., Investigations in geophysics no. 6.

Wang, Z., Hirsche, W.K., and Sedgwick, G., 1991, Seismic velocities in carbonate rocks: J. Can. Petr. Tech., 30, 112-122.

Wilkens, R., Simmons, G., and Caruso, L., 1984, The ratio *Vp/Vs* as a discriminant of composition for siliceous limestones: Geophysics, 49, 1850-1860.

Wyllie, M.R.J., Gregory, A.R., and Gardner, L.W., 1956, Elastic wave velocities in heterogeneous and porous media: Geophysics, 21, 41-70.